Deterministic and Monte Carlo Codes for Multiple Scattering Photon Transport

Jorge E. Fernández [1,2]

(1) Laboratory of Montecuccolino (DIENCA)
Alma Mater Studiorum University of Bologna, Italy

(2) Istituto Nazionale di Fisica Nucleare (INFN)

Summary

- Introduction
- Unbiased Monte Carlo simulation of the Compton Profile
- Deterministic vs Monte Carlo codes for transport calculations of line width effects
- Electron contributions to photon transport
- Conclusions

Introduction

- Deterministic and Monte Carlo techniques compete to provide the best description of transport problems.
- However, many times they demonstrate to be complementary.
- This talk offers three examples from our experience in photon transport which illustrate the close cooperation between these two approaches.

Summary

- Introduction
- Unbiased Monte Carlo simulation of the Compton Profile
- Deterministic vs Monte Carlo codes for transport calculations of line width effects
- Electron contributions to photon transport
- Conclusions

Unbiased Monte Carlo simulation of the Compton Profile

This example shows how a deterministic calculation has been used to correct a biased Monte Carlo algorithm widely adopted to simulate the Compton profile.

ELSEVIER

Available online at www.sciencedirect.com

ScienceDirect

Nuclear Instruments and Methods in Physics Research B 263 (2007) 209 213

NIM B
Beam Interactions with Materials & Atoms

www.elsevier.com/locate/nimb

Unbiased Monte Carlo simulation of the Compton profile

J.E. Fernandez [a,b,*], V. Scot [b]

[a] National Institute of Nuclear Physics (INFN), Italy
[b] National Institute for Physics of Matter (CNR/INFM) and Laboratory of Montecuccolino-DIENCA, Alma Mater Studiorum University of Bologna, Bologna, Italy

Compton profile

- It is the broadening of the Compton peak
- It is produced by the momentum distribution of the electrons in the atom
- it can be measured quite precisely in synchrotron facilities

Biased Algorithm

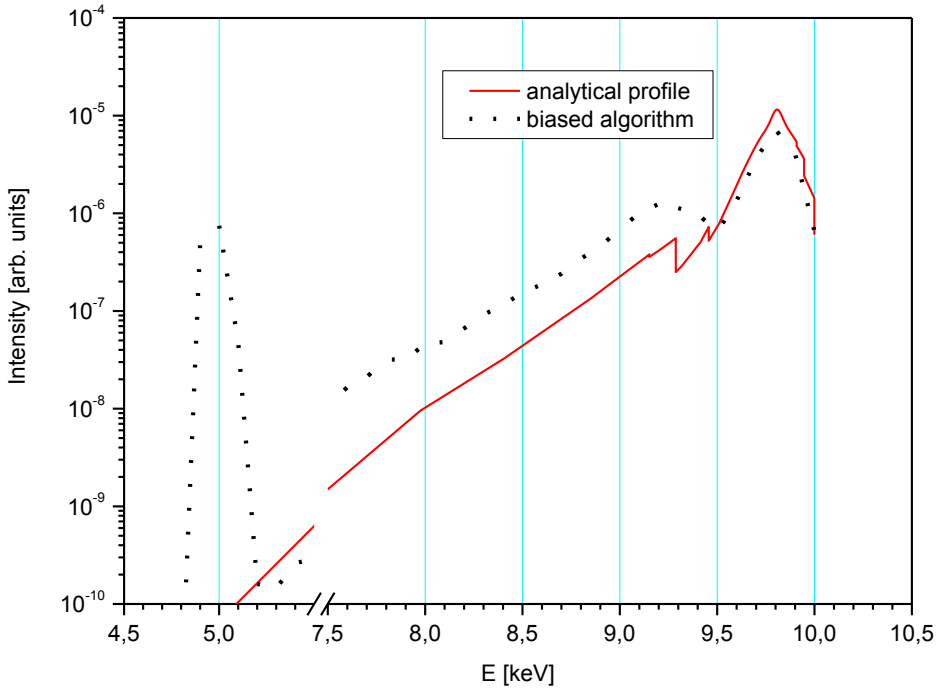

It was discovered a biased behaviour in Compton profile MC simulation (at low energies) when using the standard algorithm by Namito[1] (used by EGS and MCNP)

The bias was responsible for:

- the creation of a false peak in correspondence with the low energy tail of the profile
- a wrong Compton profile at low energies

[1] Y.Namito, S.Ban, H.Hirayama,NIM A 349 (1994) 489.

Reason for the bias

Wrong sampling of the atomic sub-shells:

$$\frac{n_i}{\left(\sum_{i=1}^{shellnumber} n_i\right)}$$

sub-shells were assumed complete

i.e. having n_i electrons

Unbiased sampling

Correct sampling of the atomic sub-shells:

$$\frac{n_i \int_{-\infty}^{Q_{i,\max}} J_i(Q)dQ}{\sum_{i=1}^{shellnumber} n_i \int_{-\infty}^{Q_{i,\max}} J_i(Q)dQ}$$

sub-shells now are assumed incomplete

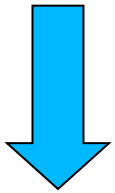

i.e. having $n_i \int_{-\infty}^{Q_{i,\max}} J_i(Q)dQ$ electrons

Results of the unbiased algorithm

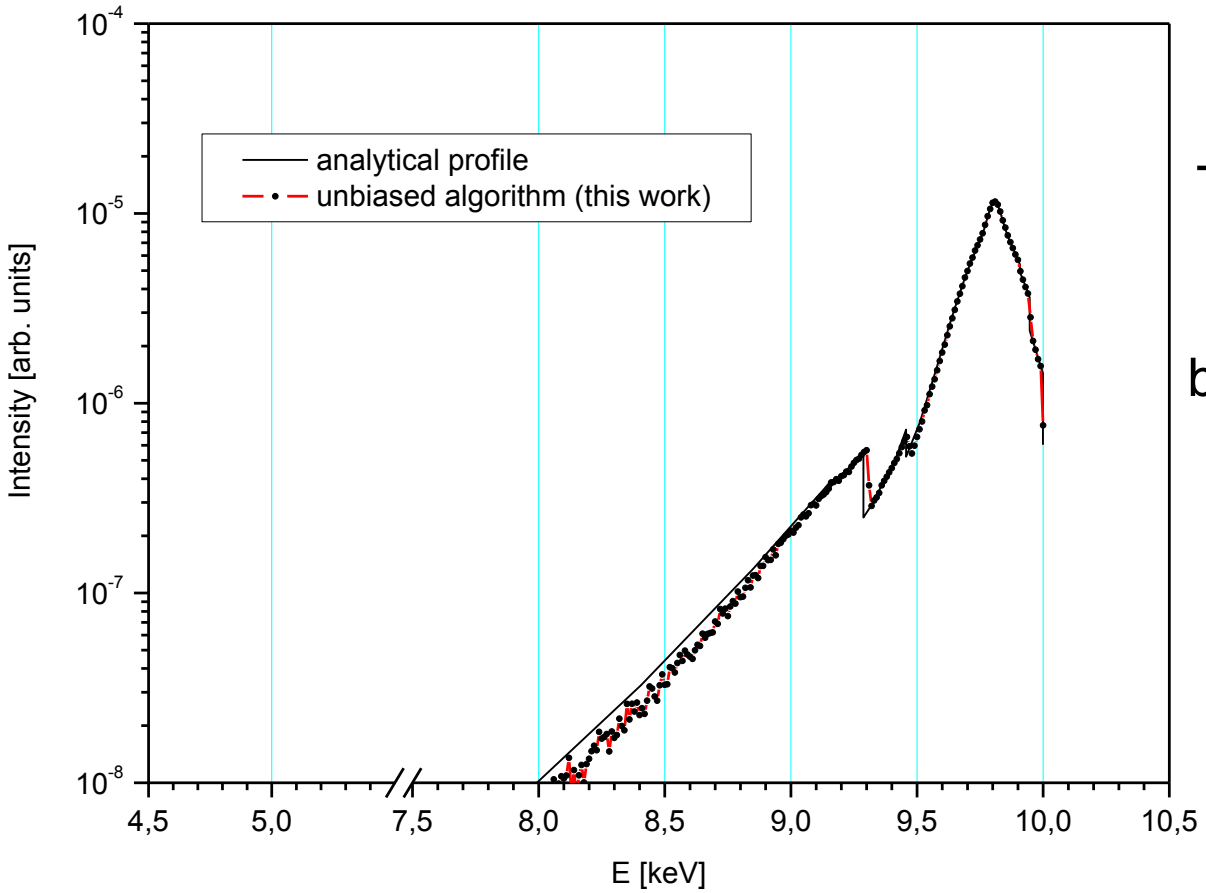

The deterministic code was essential to discover the wrong behaviour of the biased algorithm.

Summary

- Introduction
- Unbiased Monte Carlo simulation of the Compton Profile
- Deterministic vs Monte Carlo codes for transport calculations of line width effects
- Electron contributions to photon transport
- Conclusions

Condition to fulfill in order to produce photoelectric effect

$$E_0 \geq E_{absorption\ \ edge}$$

Mechanism for producing XRF lines

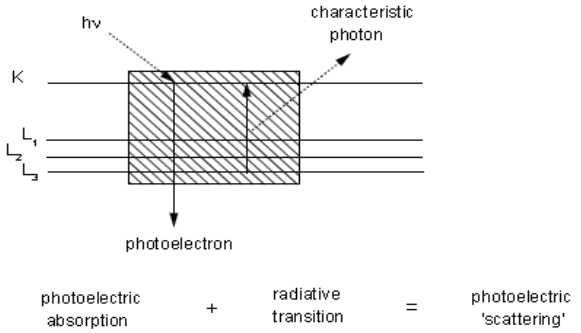

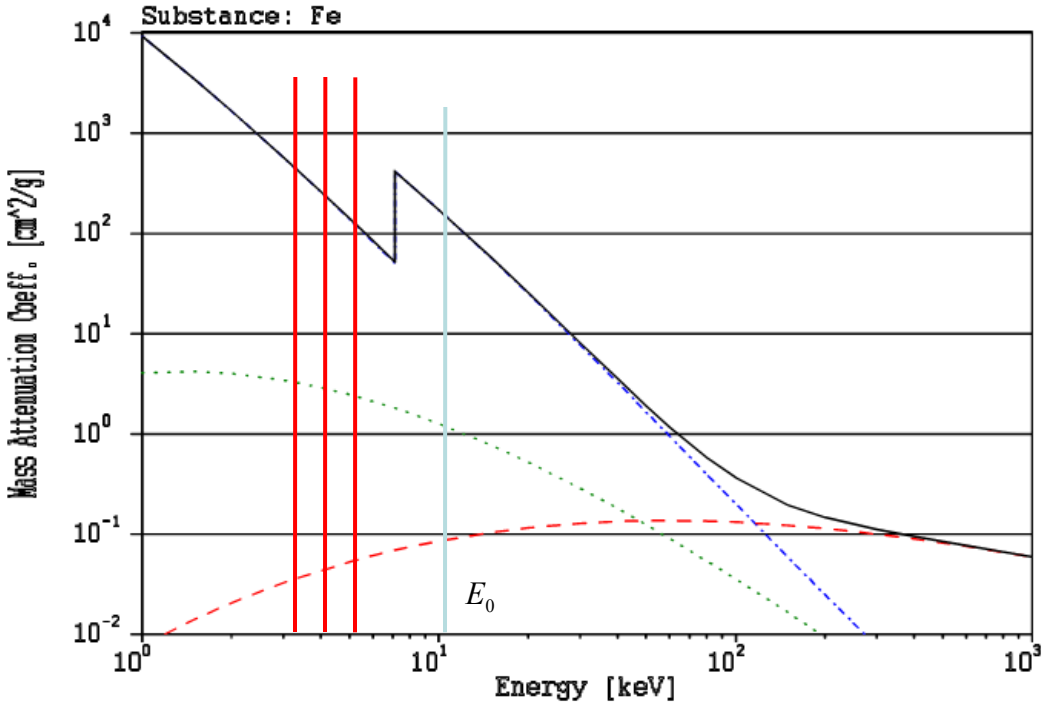

The width of the atomic levels is responsible for the natural width of the lines

$$\underbrace{\Gamma}_{\substack{total\\ transition\\ width}} = \sum_k \underbrace{\Gamma_k}_{\substack{subshell\\ level\\ width}}$$

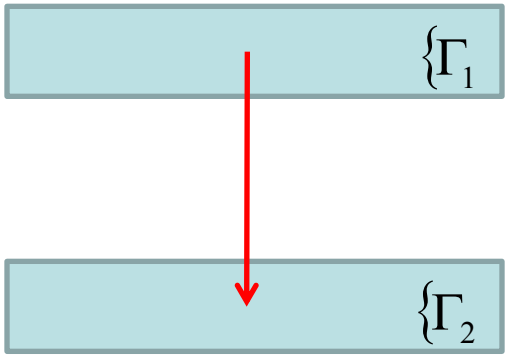

$$\Gamma = \Gamma_1 + \Gamma_2$$

The widths of the atomic levels are the recommended values in Campbell and Papp, *At. Data and Nucl. Data Tables* **77**, 1–56 (2001)

Lorentzian shape of the line

$$\ell(E, E_\ell; \gamma_{E_\ell}) = \frac{1}{\pi} \frac{\frac{\Gamma_{E_\ell}}{2}}{\left((E - E_\ell)^2 + \left(\frac{\Gamma_{E_\ell}}{2} \right)^2 \right)} = \frac{1}{\pi} \frac{\gamma_{E_\ell}}{\left((E - E_\ell)^2 + \gamma_{E_\ell}{}^2 \right)}$$

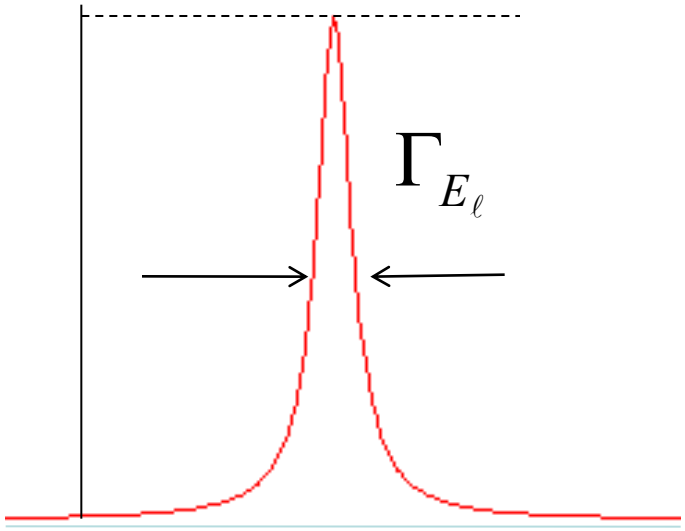

sometimes is used the
Half Width at Half Maximum (HWHM)

$$\gamma_{E_\ell} = \Gamma_{E_\ell} / 2$$

Emission of a Lorentzian K-line

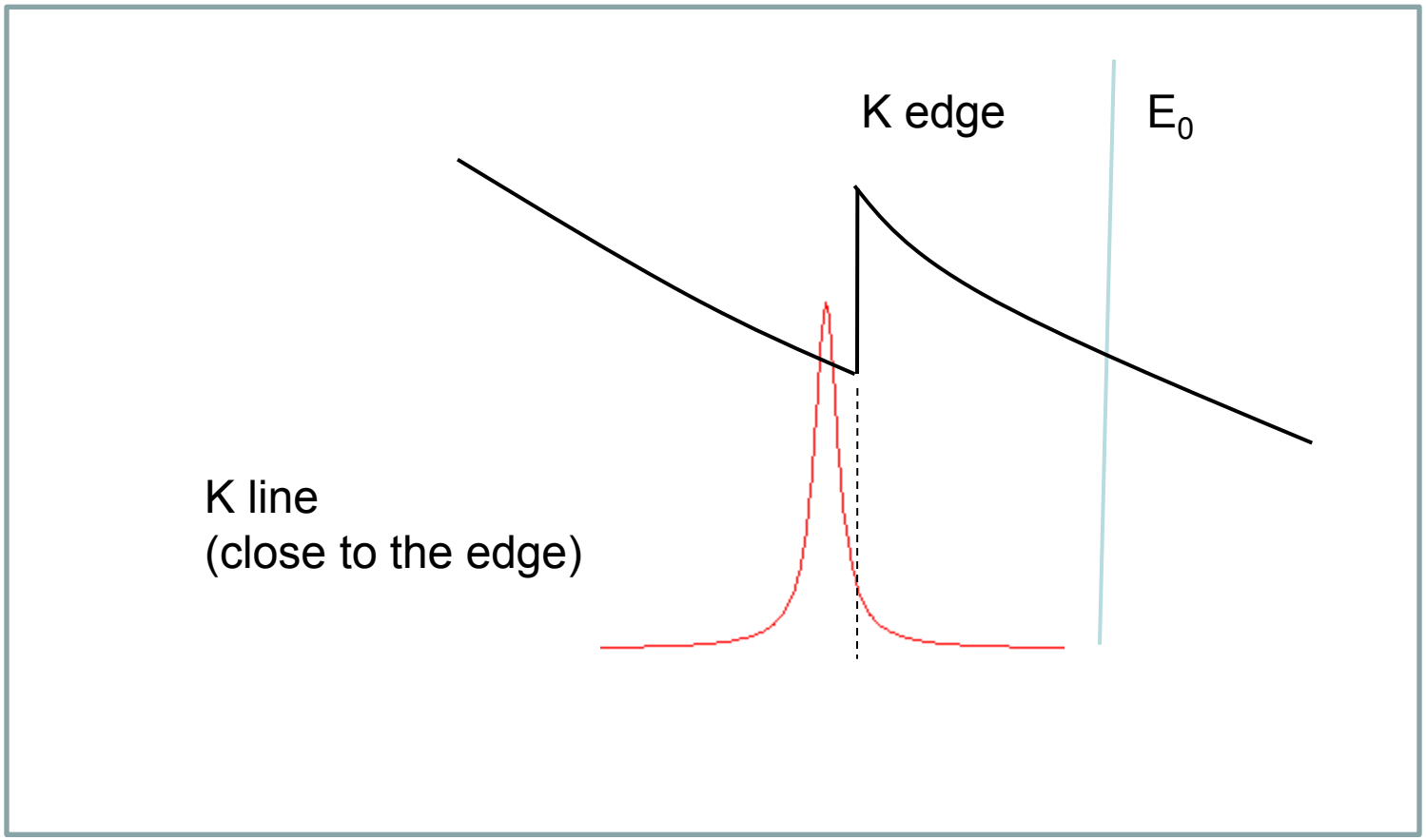

Transport kernel for a Lorentzian line (wavelength regime)

$$k_{P_{\lambda_i}}(\vec{\omega},\lambda,\vec{\omega}',\lambda')\Big|_L = \frac{1}{4\pi} Q_{\lambda_i}(\lambda')\,\ell(\lambda,\lambda_i;\gamma_{\lambda_i})\,[1-\mathrm{U}(\lambda'-\lambda_{e_i})]\,\mathrm{U}(\lambda-\lambda')$$

Emission probability

$$Q_{\lambda_i}(\lambda') = \tau_s(\lambda') g_{e_i} p_{\lambda_i}$$

Energy conservation

Threshold for photoelectric effect

edge E_0

Lorentzian distribution

$$\ell(\lambda,\lambda_i;\gamma_{\lambda_i}) = \frac{1}{\pi}\frac{\gamma_{\lambda_i}}{\left((\lambda-\lambda_i)^2+\gamma_{\lambda_i}^{\,2}\right)}$$

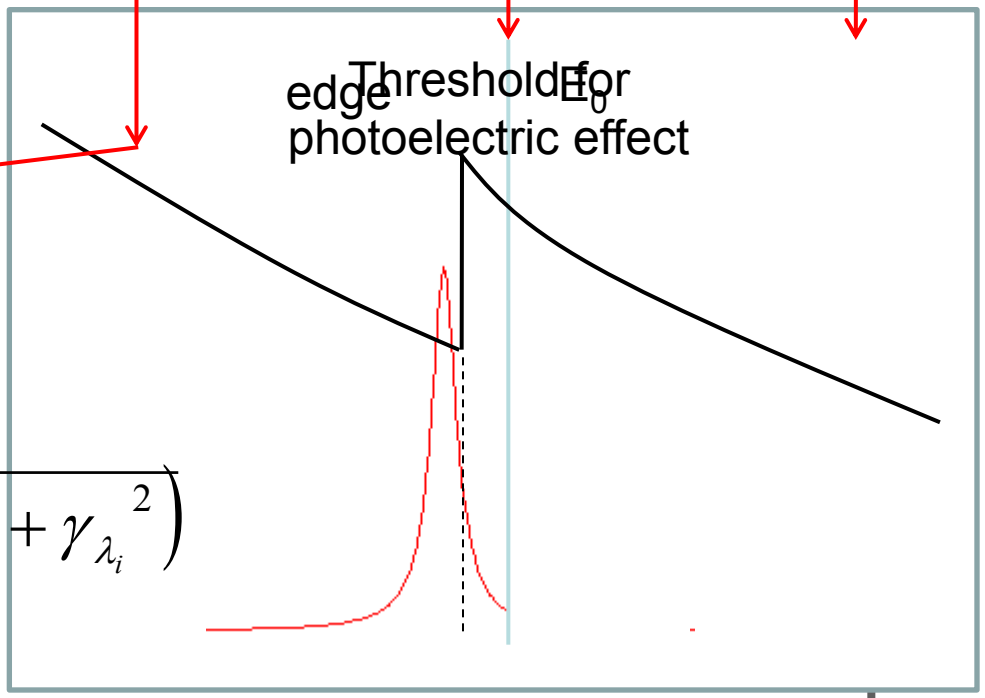

MC vs Deterministic description of a Lorentzian line

✓In MC the energy of the characteristic photon is randomly sampled at every interaction using a Lorentzian distribution centered at E_0.

✓One interesting effect appears when the Lorentzian tail crosses the edge, i.e. the energy of the emitted photon is high enough to produce another vacancy and, therefore, a self-enhancement effect.

✓Since the high energy tail has always a very low probability, this case requires refined variance reduction techniques in order to get significant results.

✓The slow asymptotic decrease of the Lorentzian distribution introduces a further complication to describe multiple scattering with reasonable statistics.

✓Therefore, we propose to use instead a deterministic method based on the wavelength (energy) discretization of the Lorentzian distribution.

Discretization of the Lorentzian distribution (wavelength regime)

We define a new normalized distribution between the finite limits $\left[-(2t+1)\gamma_i,(2t+1)\gamma_i\right]$

$$\ell_\nu(\lambda,\lambda_i;\gamma_{\lambda_i}) = \frac{1}{\nu\pi}\frac{\gamma_{\lambda_i}}{\left((\lambda-\lambda_i)^2+\gamma_{\lambda_i}{}^2\right)}$$

where $$\nu = \int_{\lambda_i-(2t+1)\gamma_i}^{\lambda_i+(2t+1)\gamma_i} \ell(\lambda,\lambda_i;\gamma_{\lambda_i})\,d\lambda = \frac{2}{\pi}\arctan(2t+1)$$

and use a discrete δ-expansion for the Lorentzian

$$\ell_\nu(\lambda,\lambda_i;\gamma_{\lambda_i}) = \sum_{k=-t}^{t} p_k\ \delta\left(\lambda-\left[\lambda_i+2k\gamma_i\right]\right)$$

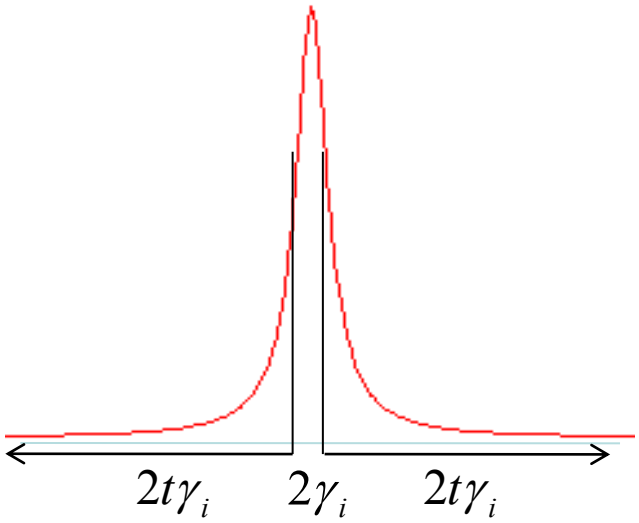

with coefficients

$$p_k = \int_{\lambda_i+2k\gamma_i-\gamma_i}^{\lambda_i+2k\gamma_i+\gamma_i} \ell_\nu(\lambda,\lambda_i;\gamma_{\lambda_i})\,d\lambda$$

$$= \frac{1}{\nu\pi}\left[\arctan(2k+1)-\arctan(2k-1)\right] \quad , \quad (k=-t..t)$$

Discretized kernel for the Lorentzian line (wavelength regime)

$$k_{P_{\lambda_i}}(\vec{\omega},\lambda,\vec{\omega}',\lambda')\Big|_L = \frac{1}{4\pi} Q_{\lambda_i}(\lambda') \sum_{k=-t}^{t} p_k \, \delta(\lambda - \lambda_{ik}) [1 - \mathrm{U}(\lambda' - \lambda_{e_i})] \mathrm{U}(\lambda - \lambda')$$

$$= \frac{1}{4\pi} Q_{\lambda_i}(\lambda') [1 - \mathrm{U}(\lambda' - \lambda_{e_i})] \sum_{k=k_{\min}}^{t} p_k \, \delta(\lambda - \lambda_{ik})$$

with

$$\lambda_{ik} = \lambda_i + 2k\gamma_i$$

$$k_{\min} = \max\left[-t, -\left|\frac{\lambda_i - \lambda'}{2\gamma_i}\right|\right]$$

(energy conservation cut-off)

Primary XRF intensity of a Lorentzian line

The primary intensity of the line centered at the peak wavelength λ_i for an infinite thickness specimen is computed within an infinitely large acquisition window

$$I_{\lambda_i}^{(1)}(0,\vec{\omega})\Big|_L = \frac{I_0}{4\pi}|\eta| Q_{\lambda_i}(\lambda_0)[1-\mathrm{U}(\lambda_0-\lambda_{e_i})]\sum_{k=k_0}^{t}\frac{p_k}{\mu_{ik}|\eta_0|+\mu_0|\eta|}$$

where

$$k_0 = \max\left[-t,-\left|\frac{\lambda_i-\lambda_0}{2\gamma_i}\right|\right]$$

$$\mu_{ik} = \mu(\lambda_{ik})$$

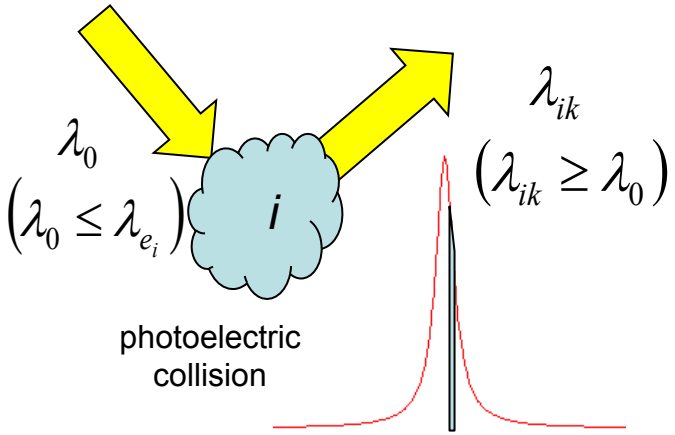

Secondary XRF intensity of a Lorentzian line

The secondary intensity of the line centered at the peak wavelength λ_i for an infinite thickness specimen is computed within an infinitely large acquisition window.

$$I_{\lambda_i}^{(2)}(0,\vec{\omega})\Big|_L = \frac{I_0}{8\pi}|\eta| \sum_{j}^{all\ lines} Q_{\lambda_j}(\lambda_0)[1-\mathrm{U}(\lambda_0-\lambda_{e_j})] \sum_{s=s\min_j(\lambda_0)}^{t} p_s\, Q_{\lambda_i}(\lambda_{js})[1-\mathrm{U}(\lambda_{js}-\lambda_{e_i})]$$

$$\sum_{k=k_{\min_i}(\lambda_{js})}^{t} \frac{p_k}{\mu_{ik}|\eta_0|+\mu_0|\eta|}\left[\frac{|\eta|}{\mu_{ik}}\ln\left(1+\frac{\mu_{ik}}{\mu_{js}|\eta|}\right)+\frac{|\eta_0|}{\mu_0}\ln\left(1+\frac{\mu_0}{\mu_{js}|\eta_0|}\right)\right]$$

$$k_{\min_i}(\lambda_{js}) = \max\left[-t,-\mathrm{Int}\left|\frac{\lambda_i-\lambda_{js}}{2\gamma_i}\right|\right]$$

$$s_{\min_j}(\lambda_0) = \max\left[-t,-\mathrm{Int}\left|\frac{\lambda_j-\lambda_0}{2\gamma_j}\right|\right]$$

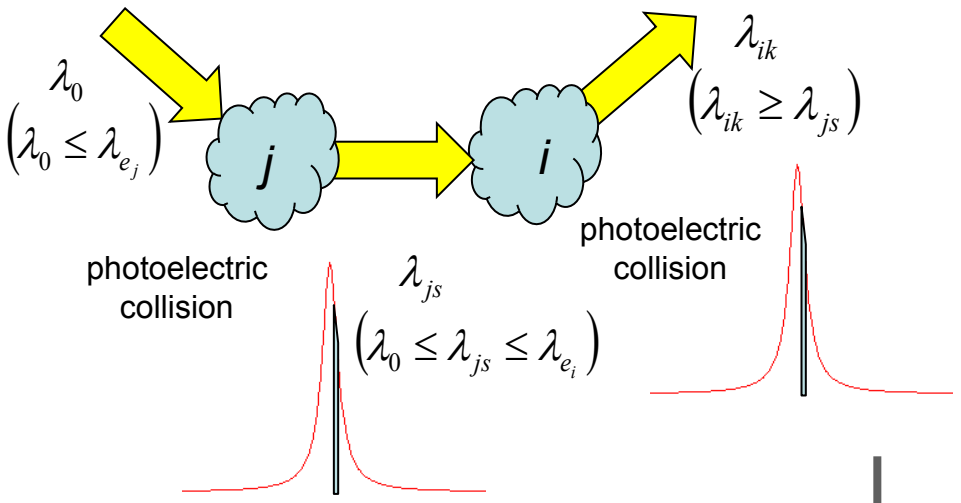

Example of almost symmetric Lorentzian lines

Sometimes the asymmetry is small …

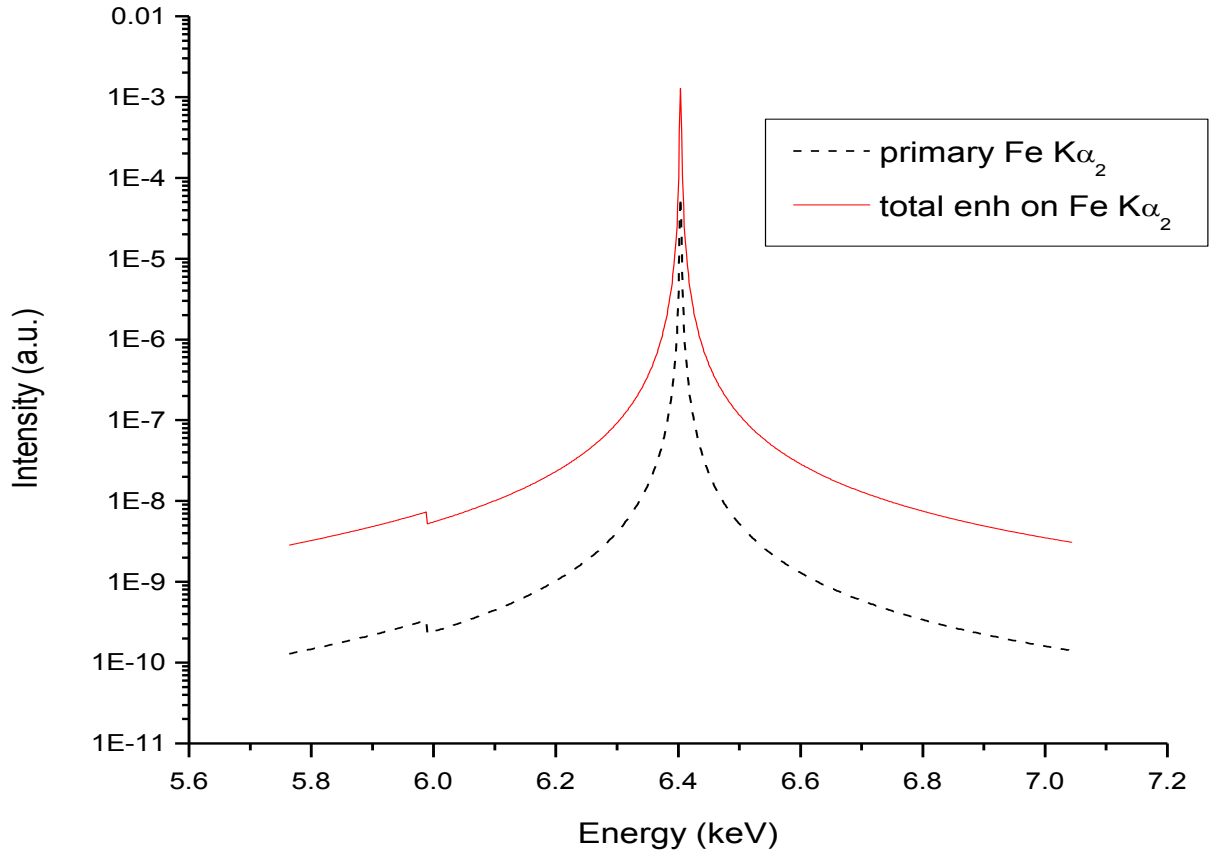

Secondary Lorentzian contributions can be very asymmetric

Sometimes the asymmetry is large …

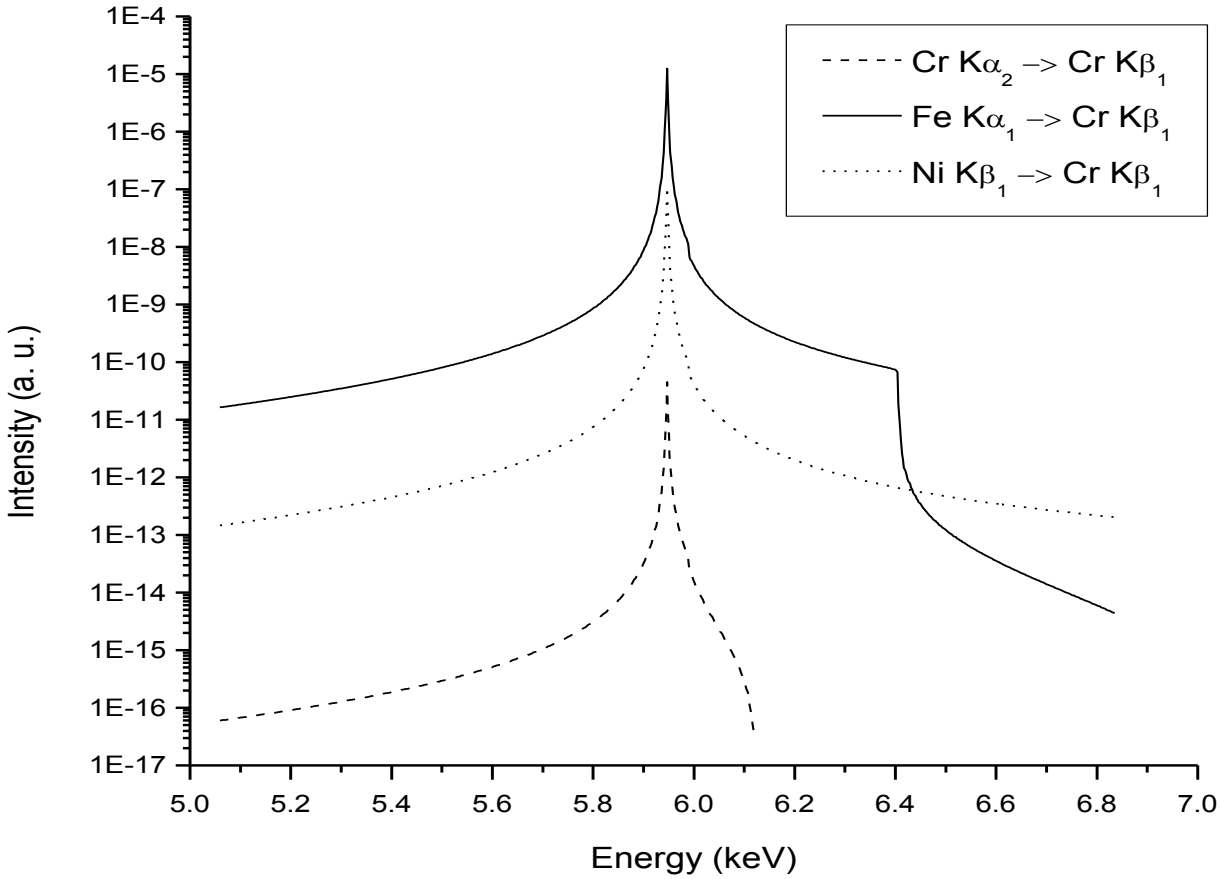

Summary

- Introduction
- Unbiased Monte Carlo simulation of the Compton Profile
- Deterministic vs Monte Carlo codes for transport calculations of line width effects
- Electron contributions to photon transport
- Conclusions

Electron contributions to photon transport

- The aim is to evaluate the contribution due to electrons to be included in photon transport codes without solving the complete coupled problem.
- The code PENELOPE (coupled electron-photon Monte Carlo) was used to study the effect of secondary electrons into the photon transport.
- The ad-hoc code KERNEL was developed to simulate a forced first collision at the origin of coordinates. We considered a point source of monochromatic photons.
- The physics of the interaction was described using the PENELOPE subroutine library.
- All the secondary electrons were followed along their multiple-scattering until their energy become lower of a predefinite threshold value.
- All photons produced by the electrons at every stage were accumulated.
- Polarization was not considered.

Prevailing photon interactions in the X-ray regime

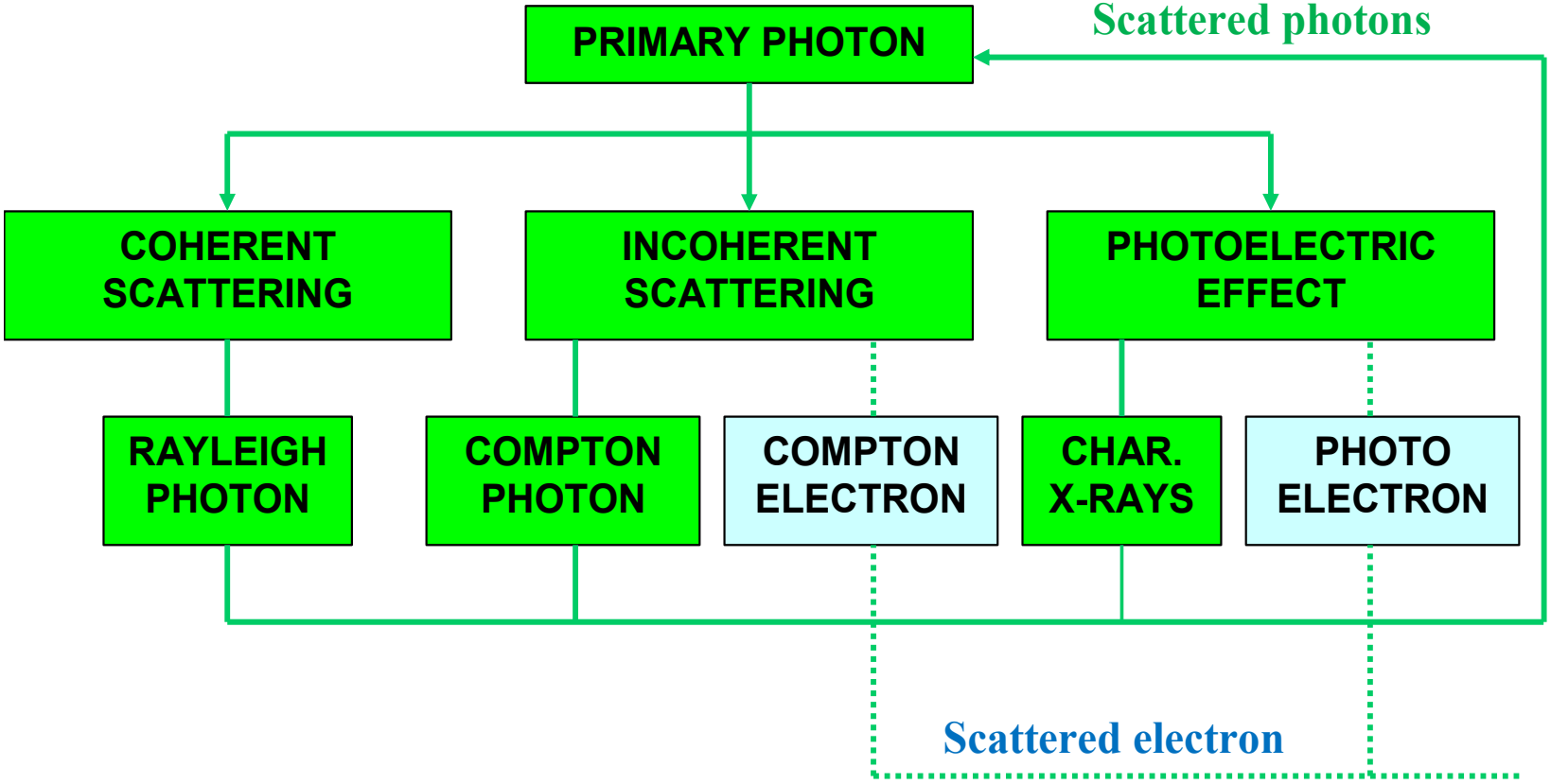

Electron-photon coupling

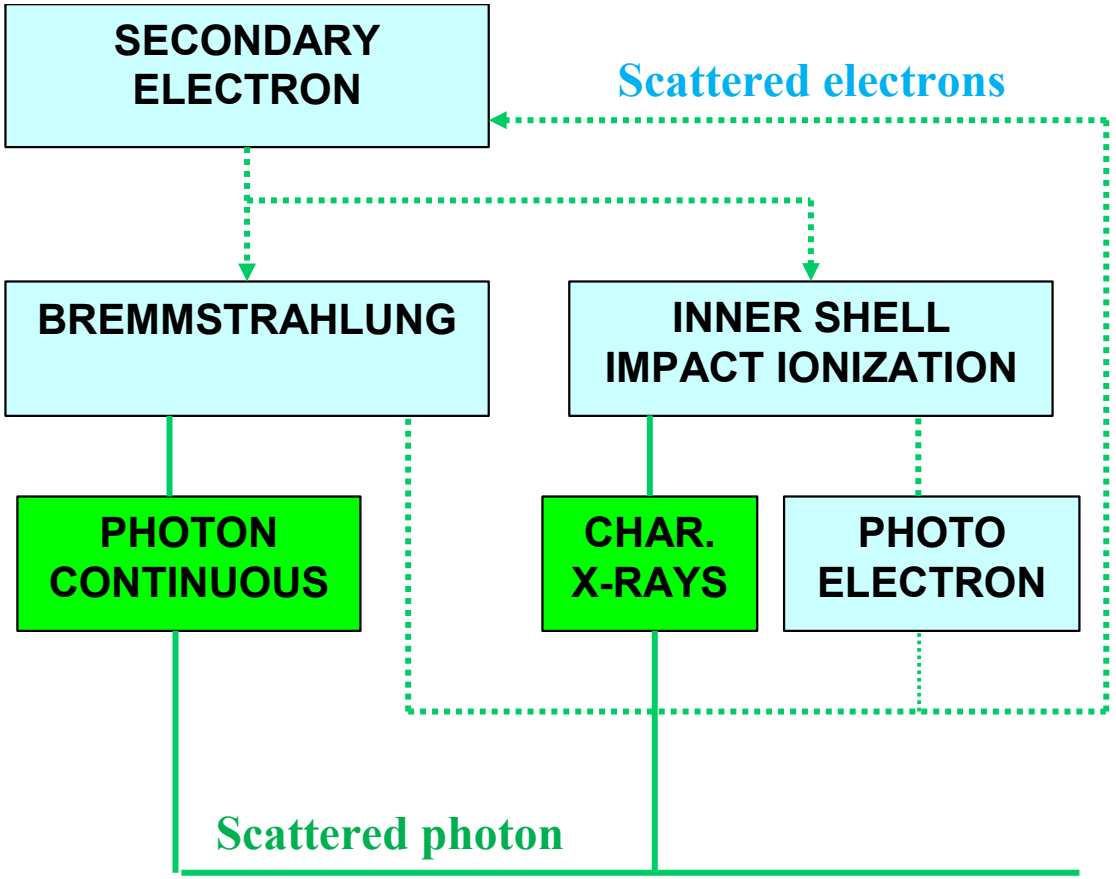

Description of the KERNEL code

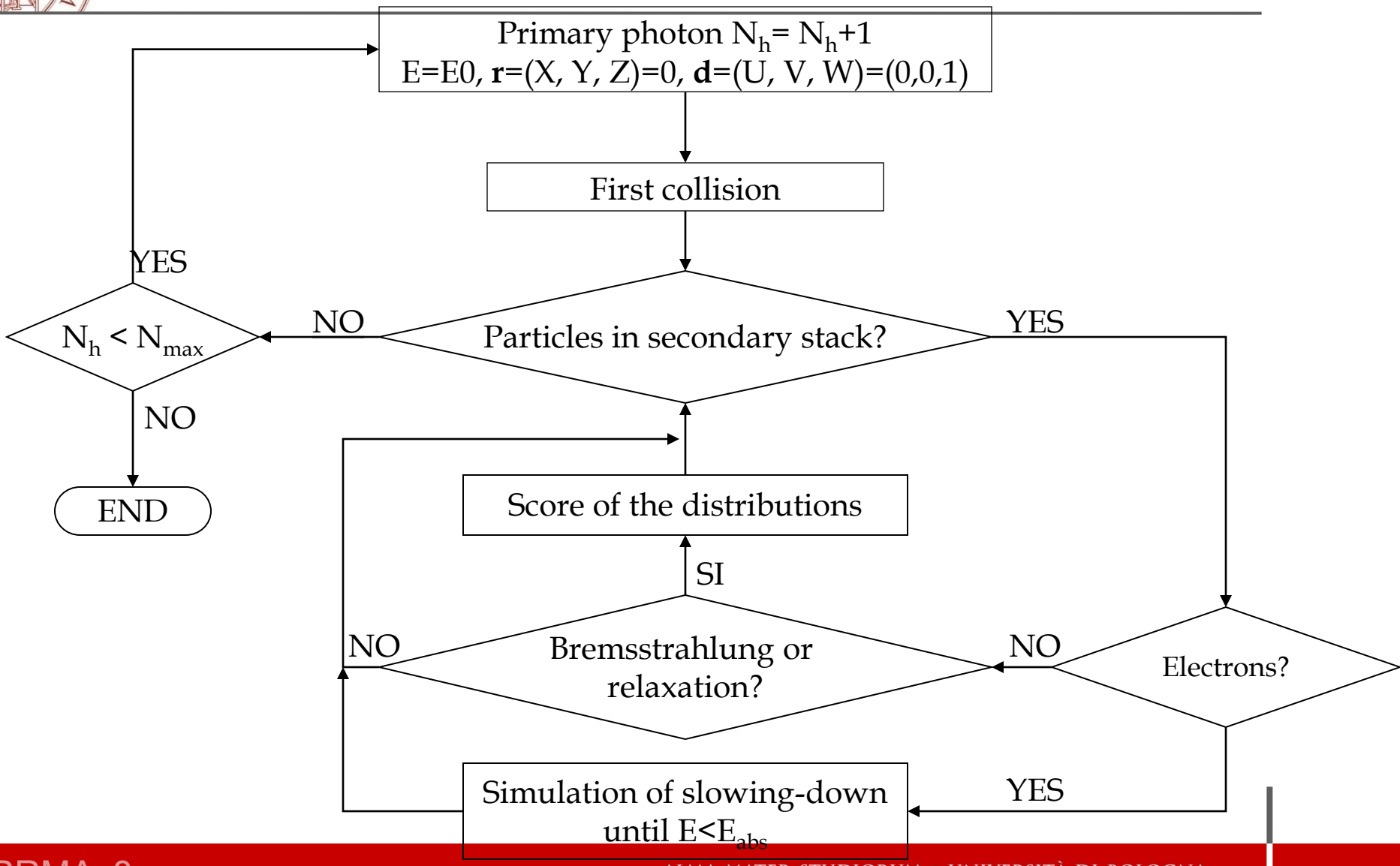

Types of electron contribution to photon transport

- Bremmstrahlung: contributes a continuous distribution

- Inner shell impact ionization: modifies the intensity of the characteristic lines

Polar angular distribution Inner-shell impact ionization

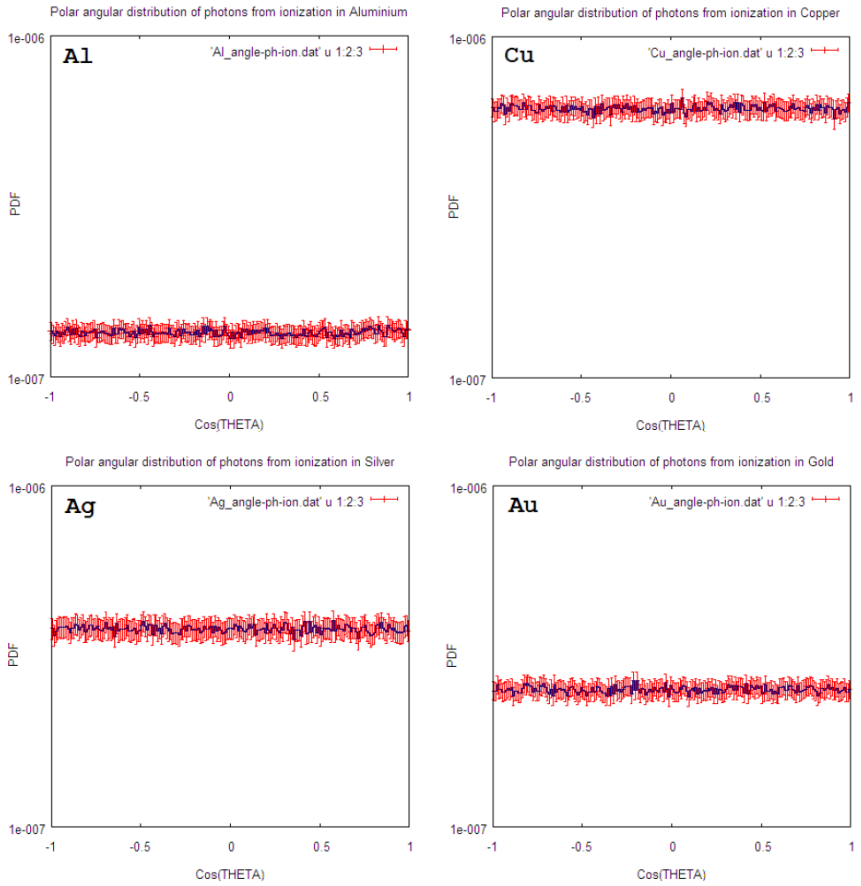

- ✓Primary photon source is 100 keV.
- ✓Blue lines denote computed values, red symbols are error bars.
- ✓The emission is isotropic.

Spatial distribution (1)
Electron range vs photon MFP

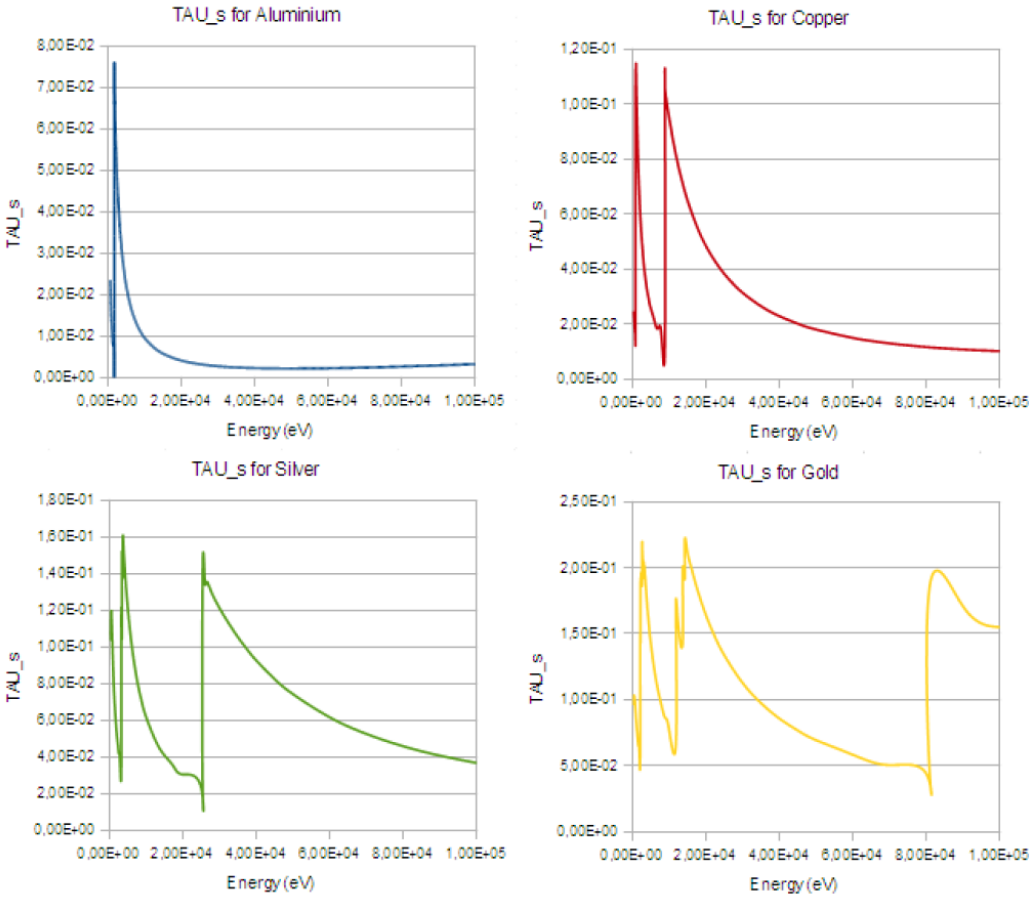

✓Parameter $\tau_s = R(E)/\lambda_p$

as a function of energy.

$R(E)$ Bethe range of electrons

λ_p Mean free-path of photons

✓Value ranges keep always small (order of 10^{-1}).

Spatial distribution (2)
Effective electron range

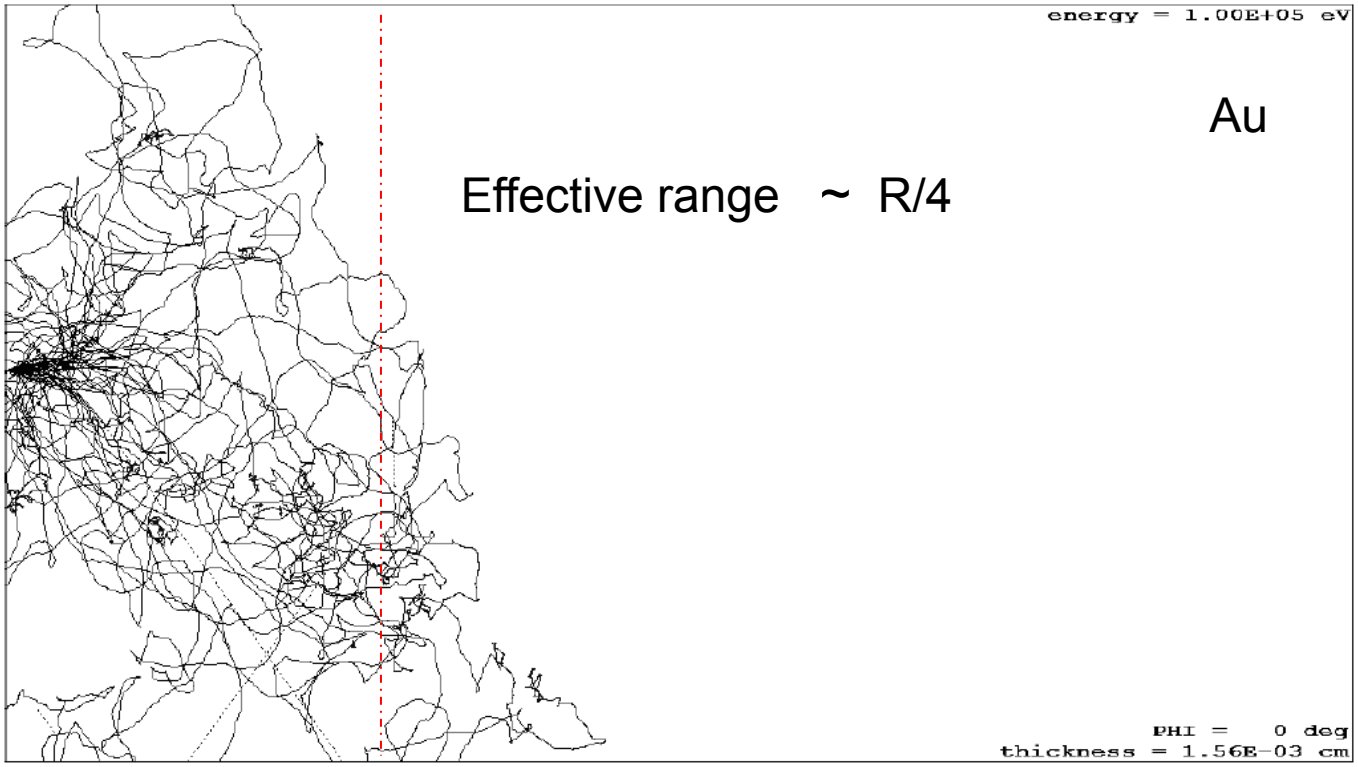

Bethe range

Photon emission
Inner shell impact ionization

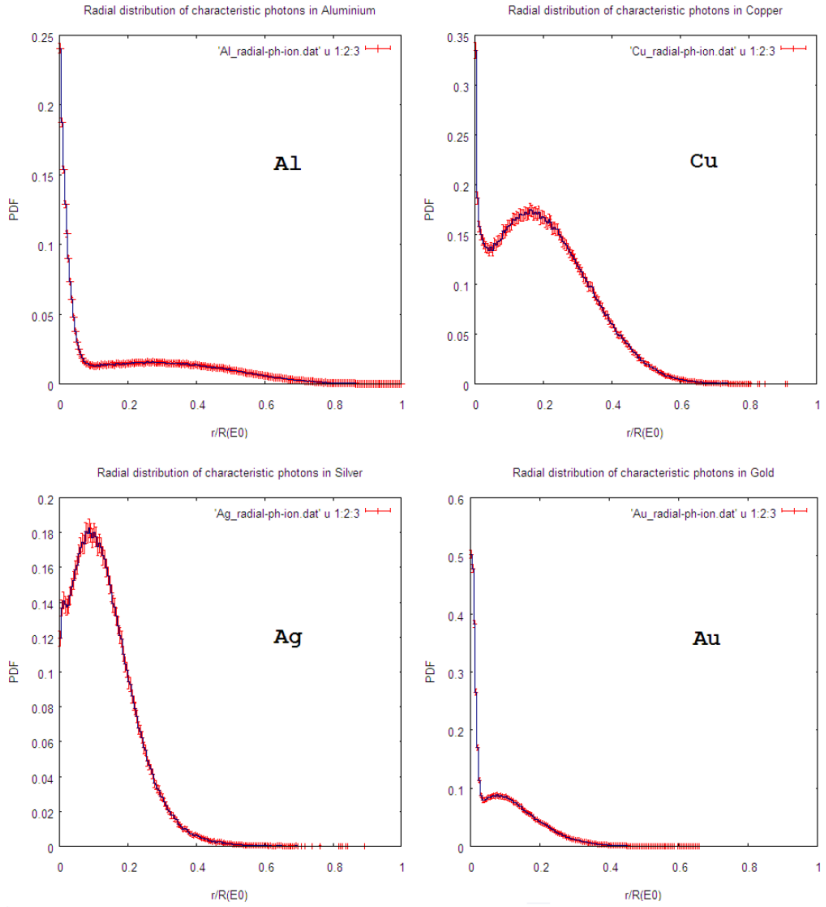

Radial distribution

✓Primary photon source is 100 keV.

✓Blue lines denote computed values, red symbols are error bars.

✓X-axis is r/R

✓All distributions keep below R/3

Photon emission
Inner shell impact ionization

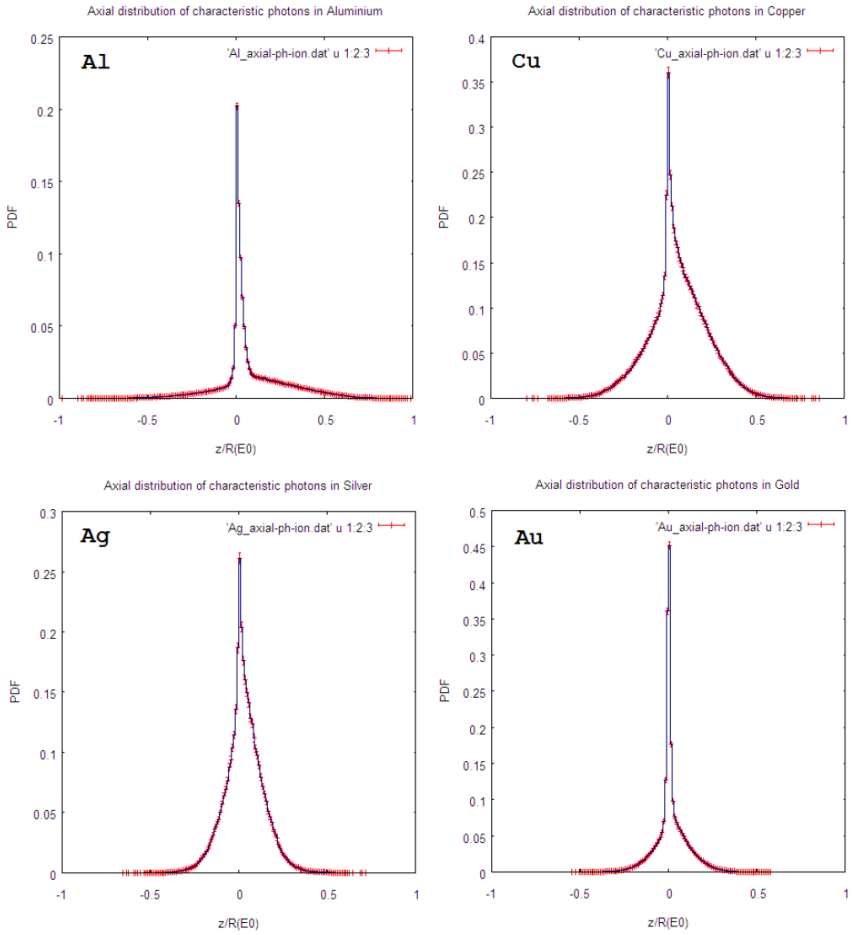

Axial distribution

✓Primary photon source is 100 keV.

✓Blue lines denote computed values, red symbols are error bars.

✓X-axis is z/R

✓All distributions keep below R/3

The correction as a function of energy

- Calculations were performed for all the lines of the elements Z=11-92 in the energy range 1-150 keV.
- Since the electrons loose their energy more efficiently in the low energy range, the computed contribution is higher for low energy lines.
- To compute the correction for a generic energy the whole interval was divided into 5 energy regions. The best fit of the energy correction at each energy interval was computed using 4 coefficients.

Electron correction on K-lines

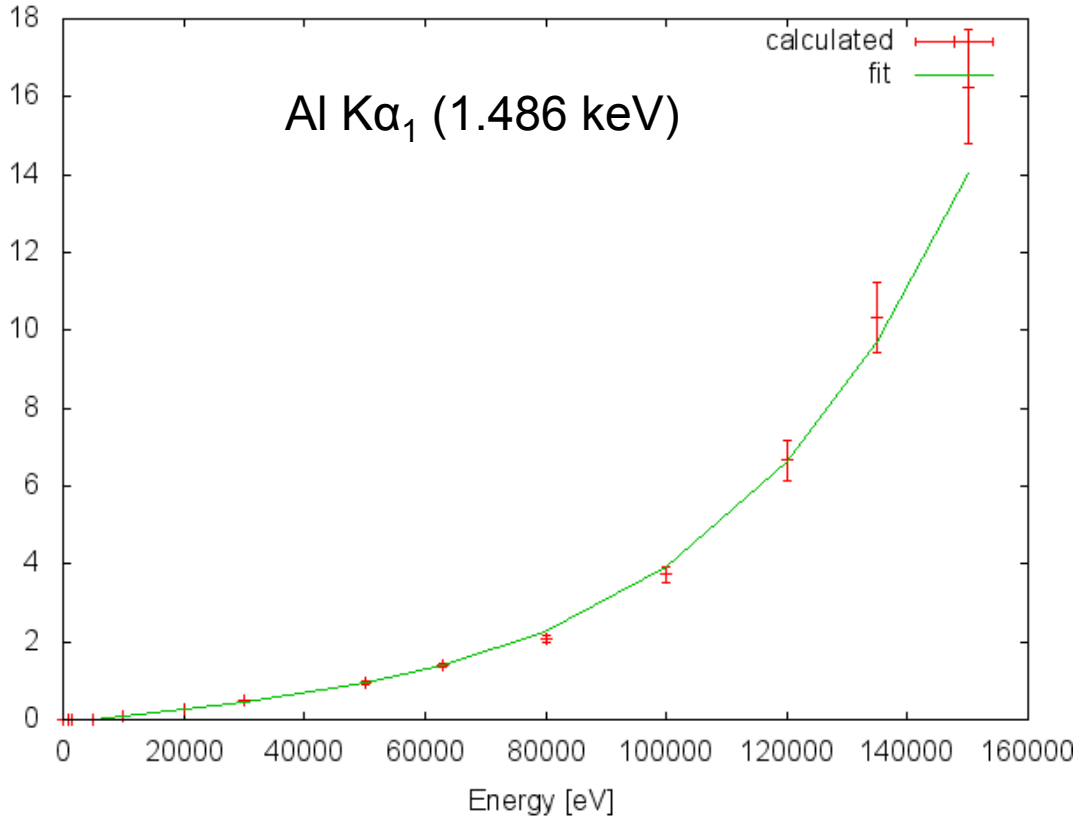

$f_{E_i}(E)\big|_{pe}$

Low Z (11-20)

Na - Ca

Best fit

$$f_{E_i}(E)\big|_{pe} = \exp\left(\sum_{k=0}^{3} \alpha_k \ln(E)^k\right)$$

Electron correction on L-lines

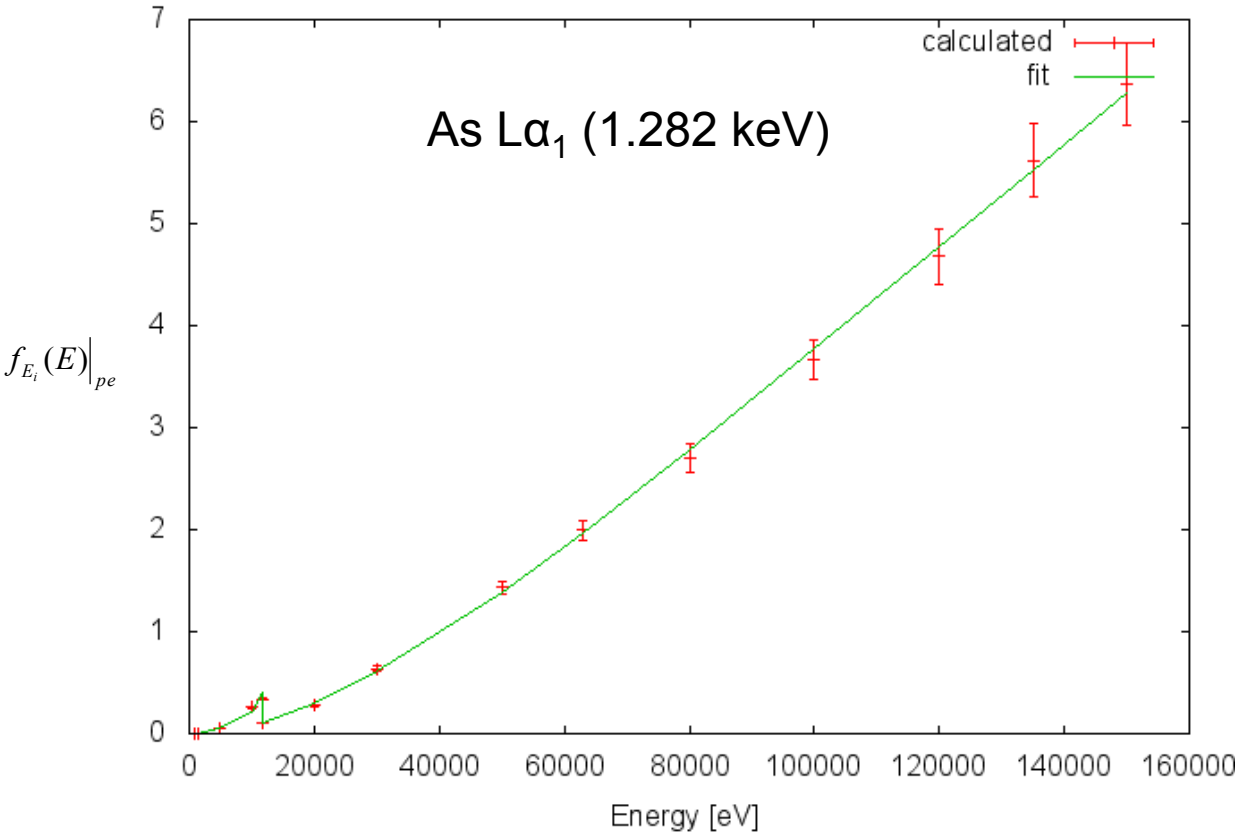

Medium Z (30-50)

Zn - Sn

Best fit

$$f_{E_i}(E)\big|_{pe} = \exp\left(\sum_{k=0}^{3} \alpha_k \ln(E)^k\right)$$

Electron correction on M-lines

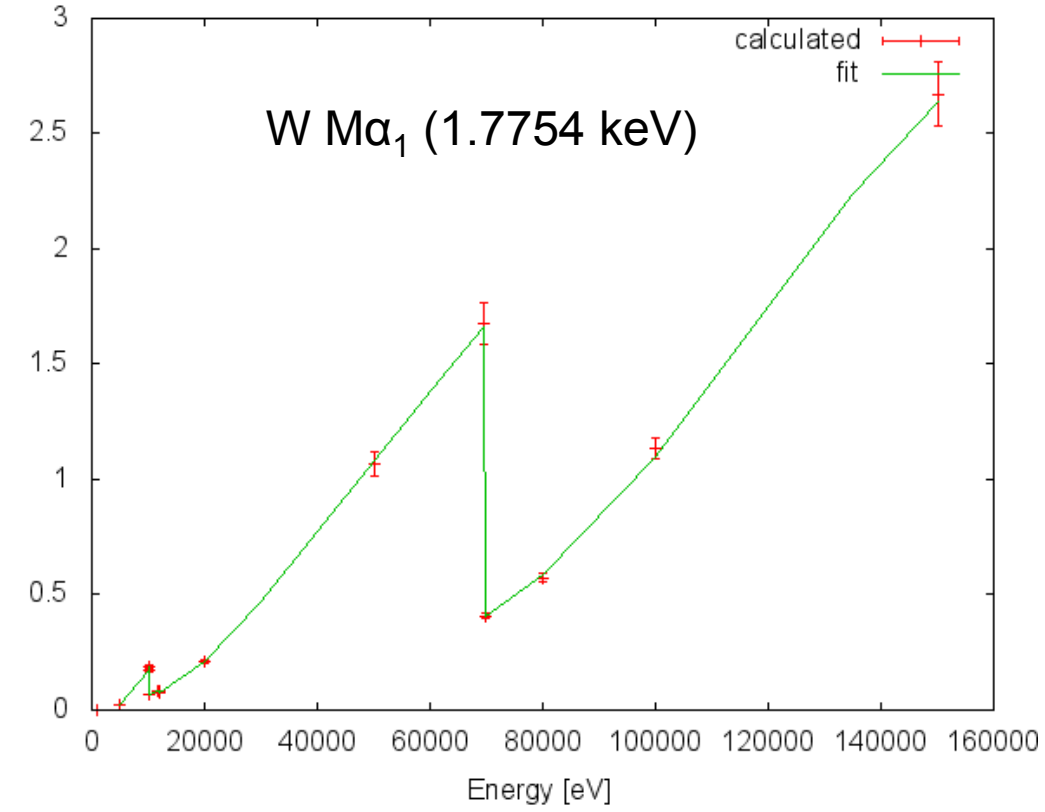

High Z (62-92)

Sm - U

Best fit

$$f_{E_i}(E)\big|_{pe} = \exp\left(\sum_{k=0}^{3} \alpha_k \ln(E)^k\right)$$

Kernel correction due to inner shell impact ionization

$$\Delta k_{P_{\lambda_i}}(\vec{\omega},\lambda,\vec{\omega}',\lambda')\Big|_{electron} = \frac{1}{4\pi} Q_{\lambda_i}(\lambda')\Big|_{electron} \delta(\lambda'-\lambda_i)\,[1-\mathrm{U}(\lambda'-\lambda_{e_i})]$$

- To avoid data-base differences between PENELOPE and other transport codes the electron correction $f_{\lambda_i}(\lambda')\big|_{pe}$ is computed in units of the photon contribution $Q_{\lambda_i}(\lambda')$.

$$\Delta k_{P_{\lambda_i}}(\vec{\omega},\lambda,\vec{\omega}',\lambda')\Big|_{electron} = \frac{1}{4\pi} \boxed{f_{\lambda_i}(\lambda')\big|_{pe}}\, Q_{\lambda_i}(\lambda')\,\delta(\lambda'-\lambda_i)\,[1-\mathrm{U}(\lambda'-\lambda_{e_i})]$$

$$f_{\lambda_i}(\lambda')\big|_{pe} = \frac{Q_{\lambda_i}(\lambda')\big|_{electron}}{Q_{\lambda_i}(\lambda')}$$

Corrected kernel comprising electron contributions

$$k_{P_{\lambda_i}}(\vec{\omega},\lambda,\vec{\omega}',\lambda') = \frac{1}{4\pi} Q_{\lambda_i}(\lambda')\left(1+ f_{\lambda_i}(\lambda')\Big|_{pe}\right)\delta(\lambda'-\lambda_i)\,[1-\mathrm{U}(\lambda'-\lambda_{e_i})]$$

where $$Q_{\lambda_i}(\lambda') = \tau_s(\lambda')\, g_{e_i}(\lambda')\, p_{\lambda_i}$$

- To compute the correction for a generic energy the whole interval is divided into 5 regions. The best fit of the energy correction at each energy interval requires 4 coefficients.

$$f_{\lambda_i}(\lambda')\Big|_{pe} = \exp\left(\sum_{k=0}^{3}\alpha_k \ln(E(\lambda'))^k\right)$$

Summary

- Introduction
- Unbiased Monte Carlo simulation of the Compton Profile
- Deterministic vs Monte Carlo codes for transport calculations of line width effects
- Electron contributions to photon transport
- Conclusions

Conclusions

Deterministic and Monte Carlo techniques demonstrate to be complementary to provide the best description of transport problems.

We have shown three different cases in photon transport to illustrate the symbiosis of MC and Deterministic approaches:

1) Deterministic calculations were essential to discover the wrong behaviour of a biased algorithm used to simulate the Compton profile in largely diffused MC codes.

2) Deterministic calculations provide a better framework to describe the influence of the Lorentzian breath on multiple scattering contributions to XRF lines.

3) Coupled photon-electron MC calculations were essential to obtain a simple correction of the photon kernel to include the effect of inner shell impact ionization from electrons.

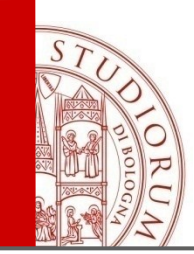

ALMA MATER STUDIORUM
UNIVERSITÀ DI BOLOGNA

Jorge Fernandez
jorge.fernandez@unibo.it